Dalton Transactions

Cite this: *Dalton Trans.*, 2012, **41**, 658

www.rsc.org/dalton

PAPER

Crystal structure, electronic properties and cytotoxic activity of palladium chloride complexes with monosubstituted pyridines†

Agnieszka Krogul,*[a] Jakub Cedrowski,[a] Katarzyna Wiktorska,[b] Wojciech P. Ozimiński,[b,c] Jadwiga Skupińska[a] and Grzegorz Litwinienko*[a]

Received 26th July 2011, Accepted 28th September 2011
DOI: 10.1039/c1dt11412c

Palladium(II) complexes attract great attention due to their remarkable catalytic and biological activity. In the present study X-ray characterization, UV-Vis and Time-Dependent Density Functional Theory (TD-DFT) calculations for six $PdCl_2(XPy)_2$ complexes (where: Py = pyridine; X = H, CH_3 or Cl) were applied in order to investigate substituent effects on their crystal structures and electronic properties and to combine the results with their catalytic and cytotoxic activity. The structures of complexes $PdCl_2(3\text{-MePy})_2$, $PdCl_2(4\text{-MePy})_2$ and $PdCl_2(2\text{-ClPy})_2$, have been described for the first time and we compared our results with available data for the whole series of six complexes. All compounds exhibit a square planar coordination geometry in which the palladium ion coordinates two nitrogen atoms of pyridine ligands and two chlorine atoms in *trans* positions. For complexes with *ortho* substituted XPy ligands a *cis* disposition of substituents takes place, whereas for other ligands: 3-MePy and 3-ClPy – the substituents are in *trans* positions. For XPy the energies of π–π* and n–π* transitions depend on the position and nature of the X substituent in the XPy ring. After complex formation a hipsochromic shift (24–34 nm) of π–π* and a bathochromic shift of n–π* bands are observed. The UV-Vis spectra of $PdCl_2(XPy)_2$ confirm that square planar coordination geometry of complexes I–VI and two dπ–π* transitions are expected. With the help of the TD-DFT calculations we proved that dπ–π* transitions in solutions of $PdCl_2(XPy)_2$ complexes result from MLCT (metal-to-ligand charge transfer) with contribution from chlorine atoms to palladium. We also studied substituent effects on cytotoxic properties of Pd(II) complexes against the human breast cancer cell line MCF7, the human prostate cancer cell line PC3, and the human T-cell lymphoblast-like cell line CCRF. The studied complexes were the most active against the CCRF cell line and less or even no cytotoxic effect was observed for PC3 cells. Complexes with MePy ligands showed increased cytotoxic activity compared to unsubstituted pyridine ligands.

Introduction

Complexes of palladium are considered as promising novel materials of wide applicability. Palladium square planar complexes with pyridine ligands are relatively ease to prepare and have remarkable catalytic activity,[1–6] thus, complexes of palladium(II) with amines are efficient catalysts for industrially important processes, *i.e.* carbonylations,[2,3] polymerizations[4] and other organic reactions like, for example, the Heck reaction, Suzuki–Miyaura cross-coupling, Sonogashira coupling, Negishi coupling, Stille cross coupling, *etc*.[5,6] Moreover, palladium(II) complexes are supposed to be potential anticancer agents and this expectation flows from a close resemblance of Pd complexes to Pt complexes.[7] The most recognized anticancer agent is *cis*-diamminedichloroplatinum(II), a compound colloquially named cisplatin. Unfortunately, therapeutic application of cisplatin has been limited by its serious side effects like, for example, nephrotoxicity, ototoxicity, neurotoxicity, allergy. An additional reason which has limited the applicability of Pt complexes is that some kinds of tumor cells (*i.e.* ovarian or small cell lung cancers) have shown a resistance after initial treatment with cisplatin.[8,9] This kind of chemoresistance has been also observed by Reedijk *et al.*[10] for other Pt complexes (being simple analogs of cisplatin). Recently, some attention has been focused on compounds with bulky planar ligands which are believed to be kinetically and thermodynamically more stable than simple

[a]*University of Warsaw, Pasteura 1, 02-093, Warsaw, Poland. E-mail: litwin@chem.uw.edu.pl, akrogul@chem.uw.edu.pl; Fax: (48) 22 8222380; Tel: (48) 22 8220211 ext. 378*
[b]*National Medicines Institute, Chelmska 30/34, 00-725, Warsaw, Poland*
[c]*Institute of Nuclear Chemistry and Technology, Dorodna 16, 03-195, Warsaw, Poland*

† Electronic supplementary information (ESI) available: Elemental analysis of complexes **I**, **II** and **VI**. Structures of complexes **III–V**. Selected bond distances and angles for complexes **III–V**. UV-Vis spectra of free XPy ligands and $PdCl_2(XPy)_2$ complexes. Frontier Orbitals involved in dπ–π* transitions in complexes **I** and **VI**. Visualisation of dπ–π* transitions in complexes **I** and **VI**. Theoretical UV-Vis spectra of complexes **I**, **III** and **VI**. CCDC reference numbers 837204–837206. For ESI and crystallographic data in CIF or other electronic format see DOI: 10.1039/c1dt11412c

analogs of cisplatin.[11] Most of the therapeutically investigated complexes are *cis* isomers although sometimes *trans* conformers also demonstrate high activity.[12] Noticeable cytotoxic activity, comparable to standard platinum-based anticancer agents, was exhibited by some planar *trans* aminepalladium(II) complexes *i.e.* *trans*-$PdCl_2L_2$ (where L = hydroxypyridine substituted in the 2-, 3- or 4- position).[13] Thus, design, synthesis and studies on anticancer properties of *trans* palladium complexes are based on assumptions that complexes with the new metal in the coordination center will exhibit remarkable antitumor activity with less side effects.[13] Indeed, there is a general agreement that DNA can be protected not only by Pt(II) but also by Pd(II).[14] Taking into account all the above mentioned arguments, a particular interest has been located on palladium(II) complexes with planar amines where steric and electronic features of ligands may affect the mechanism of substitution at the metal centre and DNA binding. Pd(II) complexes with pyridine-type ligands, (*e.g.* pyrazole)[11] and some other complexes, for example with 2,6-dimethyl-4-nitro-pyridine ligand, reveal better cytotoxic properties than cisplatin.[7]

Coordination compounds of palladium(II) are model substrates for studies on crystal geometry of square planar complexes. Since the catalytic and cytotoxic activity of these complexes depends on their electronic and crystal structure[15,16] an introduction of different ligands to the coordination sphere is a simple and convenient method that allows the steric and electronic environment to be modulated around the metal centre[17] leading to an improvement in the desired properties of a modified complex. Recently, much effort has been devoted to the synthesis of new palladium complexes with relatively complicated multifunctional ligands such as pincer groups,[17] multidentate pyridine-type ligands like bis(2-pyridylmethyl)amine,[18] pseudorotaxanes,[19] or a combination of nitrogen donor – pyridine and *N*-heterocyclic carbene. These complexes display intriguing coordination chemistry and effective catalytic activities,[6] however, full characterization of simple complexes allows for improved design and synthesis of much more advanced compounds. Although in the early sixties and seventies of the last century the transition metal(II) halides complexes with pyridine were extensively studied, the coordination geometry and electronic properties for the series of palladium(II) complexes with simple ligands *i.e.* MX_2L_2 (where: M is metal, X is halide and L is pyridine or its derivative) still remain unexplored.[20] This part of physical organometallic chemistry is unrecognized though detailed, systematic studies on simple Pd(II) complexes appear as an interesting area potentially resulting in data that might be applied to design new compounds with higher antitumor and higher catalytic efficiency.

Pyridine and its derivatives are often regarded as model compounds for studies of more complicated N-donor heterocyclic ligands and many natural heterocyclic amines are based on pyridine rings – the most prominent and most important derivatives such as nicotine, nicotinamide and nicotinamide adenine dinucleotide diphosphate (NADP) or pyridoxine (vitamin B_6) occupy key positions in biochemistry.[21–23] A pyridine-type ring is also an important building block of the purine system, which co-forms DNA and plays a substantial role in cell division. Therefore, a combination of pyridine derivatives with palladium to form Pd(II) complexes are supposed to have a large affinity for DNA binding sites.[11]

Our studies have long been concerned with the structural effects of substrates on the yield of carbonylation of amines and nitrocompounds.[24–28] We described the substituent effects in the nitrobenzene and aniline ring on the yield of ethyl *N*-fenylcarbamate (EPC) in the carbonylation of a nitrobenzene (NB), mixture NB/AN or AN (where AN is aniline), respectively.[29,30] However, our previous studies were limited to $PdCl_2$ and $PdCl_2Py_2$ complexes without detailed research on the nature of a ligand and structure of a catalyst. Recently, we have focused on the synthesis and catalytic activity of palladium(II) chloride complexes with pyridine and its derivatives in the carbonylation of nitrobenzene.[1] High turnover numbers were observed for complexes dependent on a ligand present in the complex. We observed a correlation between the catalytic activity of $PdCl_2(X_nPy)_2$ complexes (where: X = Cl or CH_3, n = 0–2) and electron density on the nitrogen atom in a pyridine ligand—described by the basicity of X_nPy. Moreover, incorporation of *ortho*-substituted pyridines to palladium catalyst decreased the yield of the investigated reaction.[1] Based on our results we proposed the mechanism of carbonylation of NB where electron transfer from the palladium atom to nitrobenzene is the rate determining step.[1] During previous studies we realized that, according to our knowledge, no detailed systematic analysis of the absorption spectra of square planar palladium(II) complexes with substituted pyridines had been reported. Therefore, we decided to compare crystal structures and electronic properties of a series of six $PdCl_2(XPy)_2$ (where: X = H, CH_3 or Cl) complexes to investigate substituent effects on structural and spectral properties and to combine the results with catalytic and biological activity of these complexes.

Results and Discussion

In order to investigate substituent effects on structural and electronic properties of Pd(II) complexes we prepared model compounds formed from $PdCl_2$ and pyridine derivatives containing methyl and chlorine substituents. In our previous work we showed that $PdCl_2(X_nPy)_2$ (where: X = CH_3 or Cl; n = 0–2) complexes are selective catalysts in the carbonylation of nitrobenzene in the presence of the catalytic system $PdCl_2(X_nPy)_2$/Fe/I_2/X_nPy.[1] Moreover, the catalytic activity of the $PdCl_2(X_nPy)_2$ compounds depends on electronic properties and position of a substituent in the pyridine ring – higher conversions of NB were observed for complexes with pyridines containing electron donating methyl groups and the highest turnover frequency (TOF) was observed for $PdCl_2$(4-MePy)$_2$. The electron donating/electron withdrawing properties of X_nPy ligands were described by the basicity of pyridine derivatives. We also noticed that the presence of substituents in the *ortho* position of the pyridine ring decreased the yield of the reaction. In the current studies on square planar palladium(II) complexes with substituted pyridines we decided to explore the substituent effects on molecular structure and electronic properties of the complexes in order to find a possible correlation with their catalytic and biological activity. The following $PdCl_2$ complexes with monosubstituted XPy ligands are described (with their symbols in parentheses): $PdCl_2(Py)_2$ (**I**), $PdCl_2$(2-MePy)$_2$ (**II**), $PdCl_2$(3-MePy)$_2$ (**III**), $PdCl_2$(4-MePy)$_2$ (**IV**), $PdCl_2$(2-ClPy)$_2$ (**V**) and $PdCl_2$(3-ClPy)$_2$ (**VI**). The results and discussion are gathered in four subsections: structure of the complexes, comparison of electronic spectra of ligands/complexes, theoretical calculations

and, finally, a description of the cytotoxic activity of the studied $PdCl_2(XPy)_2$ complexes.

Crystal structures of $PdCl_2(XPy)_2$ complexes

According to the literature, the crystallographic data for complexes **I**, **II**, and **VI** are already known. Therefore, in this work the crystal structures of three other complexes (**III**, **IV** and **V**) are described for the first time and we compared our results with available data for the whole series of six complexes. Single yellow crystals of **III**, **IV** and **V** were obtained by slow evaporation of their acetone solutions and all three compounds were found to be neutral mononuclear palladium complexes. The crystal data and details of structure refinements for these new complexes are presented in Table 1 while Table 2 contains the selected bond distances (Å) and angles (°) collected for all complexes **I–VI**.

Structure of complex **III** (Fig. 1A and Table 1) indicates that 3-methylpyridine rings show a *trans* disposition of methyl groups. The resulting crystals have been proved to belong to the triclinic space group $P\bar{1}$. Detailed analysis shows that the 3-methylpyridine ring is not orthogonal to the coordination plane (the dihedral angle is 66.57°). The square planar coordination geometry is confirmed by angles [N–Pd–Cl] = 89.47(3)° and 90.53(3)°, respectively as it has been observed for complexes **IV** and **V** (data for these complexes are listed in Table 2). Crystals of complex **IV** belong to the monoclinic space group $P2_1/n$, the crystallographic data for compound **IV** are presented in Table 1 and the structure of **IV** is shown in Fig. 1B. Also in this complex a ligand (4-methylpyridine) ring is not orthogonal to the coordination plane and the dihedral angle between the coordination plane and the ring plane is 54.58°.

Table 1 Crystal data and details of structure refinements for compounds: $PdCl_2(3\text{-}MePy)_2$ (complex **III**), $PdCl_2(4\text{-}MePy)_2$ (complex **IV**) and $PdCl_2(2\text{-}ClPy)_2$ (complex **V**)

	Complex **III**	Complex **IV**	Complex **V**
Formula	$C_{12}H_{14}Cl_2N_2Pd$	$C_{12}H_{14}Cl_2N_2Pd$	$C_{10}H_8Cl_4N_2Pd$
Weight	363.57	363.57	404.40
Crystal system	Triclinic	Monoclinic	Triclinic
Space group	$P\bar{1}$	$P2_1/n$	$P\bar{1}$
a/Å	5.7438(5)	10.4617(5)	8.2008(18)
b/Å	7.2880(8)	3.9801(2)	8.5307(18)
c/Å	8.4654(9)	15.9063(9)	10.512(2)
α	69.081(10)		91.866(17)
β	79.744(8)	98.734(4)	91.018(17)
γ	83.763(8)		115.73(2)
V (Å)[a]	325.33(6)	654.64(6)	661.7(3)
Z[b]	1	2	2
D_c/g cm^{-3}[c]	1.856	1.844	2.030
μ/cm^{-1}[d]	1.814	1.803	2.186
R[e]	0.0127(1533)	0.0140(1356)	0.0337(2321)
R_w[f]	0.0337(1581)	0.0342(1603)	0.0761(3166)

[a] V = volume of the unit cell, [b] Z = number of formula units in unit cell, [c] D = density, [d] μ = linear absorption coefficient [e] R is R-factor, [f] R_w is weighted R-factor.

The square planar coordination geometry is confirmed by [N–Pd–Cl] angles, 89.48(3)° and 90.52(3)°, respectively (see Table 2).

The palladium complex with 2-chloropyridine (compound **V**, Fig. 1C) was significantly less soluble in common organic solvents than complexes with methylpyridines. The crystals of **V** were obtained by cooling the warm acetone solution and belong to the triclinic space group $P\bar{1}$, *i.e.* to the same group as it was observed for **III**. Surprisingly, in this complex two *trans*-coordinated

Table 2 Selected bond distances (Å) and angles (°) for complexes **I–VI**[a]

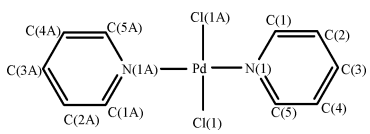

	***III–V*—this work**			***I*, *II*, *VI*—literature data**		
Bond lengths	III	IV	V	I	II	VI
Pd–N(1)[b]	2.0191(11)	2.0139(11)	2.034(3)	2.024(6)		
Pd–N(1A)	2.0191(11)	2.0139(11)	2.032(3)	2.023(6)	2.043(6)	2.010(7)
Pd–Cl(1)	2.3027(5)	2.3054(3)	2.3045(11)	2.297(1)	2.033(6)	2.010(7)
Pd–Cl(1A)[c]	2.3027(5)	2.3054(3)	2.3036(11)	2.297(1)	2.313(3)	2.315(3)
N(1)–C(1)[d]	1.3477(17)	1.3472(19)	1.405(5)	1.356(6)	2.300(3)	2.315(3)
N(1)–C(5)[e]	1.3448(17)	1.3408(18)	1.328(5)	1.356(6)	1.35(1)	1.362(10)
N(1A)–C(1A)	1.3477(17)	1.3472(19)	1.360(5)	1.336(6)	1.34(1)	1.332(10)
N(1A)–C(5A)	1.3448(17)	1.3408(18)	1.338(4)	1.336(6)	1.33(1)	1.362(10)
Bond angles						
N(1)–Pd–N(1A)	180.00	180.00(6)	178.88(12)	180.00	177.5(2)	180
N(1)–Pd–Cl(1)	89.47(3)	89.48(3)	89.32(9)	90.83(7)	90.6(2)	89.5(2)
N(1)–Pd–Cl(1A)	90.53(3)	90.52(3)	89.93(9)	90.83(7)	90.0(2)	90.5(2)
N(1A)–Pd–Cl(1)	90.53(3)	90.52(3)	91.02(9)	89.17(7)	88.7(2)	90.5(2)
N(1A)–Pd–Cl(1A)	89.47(3)	89.48(3)	89.65(9)	89.17(7)	90.6(2)	89.5(2)
Cl(1)–Pd–Cl(1A)	180.00	180.00	176.17(4)	178.3(1)	178.81(7)	180
C(1)–N(1)–Pd	119.36(9)	120.62(9)	119.7(2)	120.3(3)	117.2(5)	119.6(7)
C(5)–N(1)–Pd	121.38(9)	120.87(10)	122.3(2)	120.8(3)	123.2(5)	120.6(6)
C(1A)–N(1A)–Pd	119.36(9)	120.62(9)	117.6(2)	120.3(3)	177.5(2)	119.8(5)
C(5A)–N(1A)–Pd	121.38(9)	120.87(10)	123.8(2)	120.8(3)	90.6(2)	120.6(6)

[a] Schematic picture showing the order of the atoms. [b] N(1) corresponds to N(1B) in $PdCl_2(2\text{-}ClPy)_2$ (see Fig. 1). [c] Cl(1A) corresponds to Cl(2) in $PdCl_2(2\text{-}ClPy)_2$ (see Fig.1). [d] C(1) corresponds to C(1B) in $PdCl_2(2\text{-}ClPy)_2$ (see Fig.1). [e] C(5) corresponds to C(5B) in $PdCl_2(2\text{-}ClPy)_2$ (see Fig. 1).

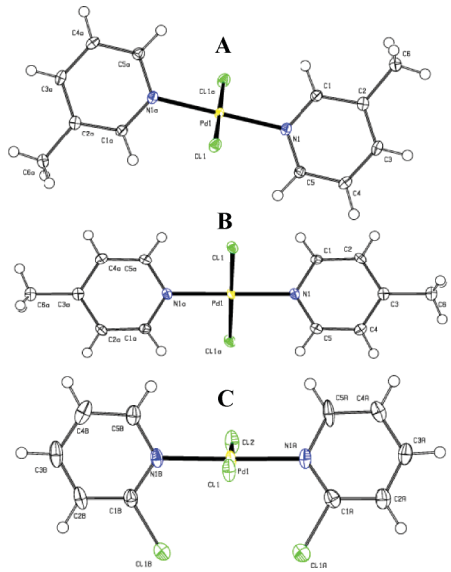

Fig. 1 SHELXL93 drawings of the molecular structures of: A) $PdCl_2(3\text{-MePy})_2$ (compound **III**), B) $PdCl_2(4\text{-MePy})_2$ (compound **IV**), C) $PdCl_2(2\text{-ClPy})_2$ (compound **V**). All drawings represent 50% probability.

2-chloroprydine rings show a *cis* disposition of the chlorine atoms and the Pd(II) ion is not located in the inversion center, on the contrary to complexes **III** and **IV**. One 2-chloropyridine ring is canted at an angle of 18.42° to the plane of another 2-chloropyridine ring and the angles formed between both the pyridine rings and the coordination plane are 86.49° and 75.09°, respectively. The angles [N–Pd–Cl] presented in Table 2 for complex **V** are close to 90° confirming its square planar coordination geometry.

Taking into account our experimental results (for compounds **III–V**) and results for the complexes **I**, **II** and **VI** (accessible in database CSD: H. Allen, *Acta Crystallogr.*, 2002, **B58**, 380),[31–33] we can state that in all six compounds the palladium ion coordinates two nitrogen atoms of pyridine ligands and two chlorine atoms in the *trans* positions, exhibiting a square planar coordination geometry. We observe either *cis* or *trans* disposition of methyl/chlorine substituents in pyridine rings. For complexes with *ortho* substituted XPy ligands a *cis* disposition of substituents takes place, whereas for other ligands: 3-MePy (complex **III**) and 3-ClPy (complex **VI**)—the substituents are in *trans* position. Consequently, complexes **III** and **VI** (with *trans* disposition of substituents in the XPy ring) as well as compounds with 4-Me (**IV**) and Py itself (**I**) have a centrosymmetric structure with the palladium atom located in the inversion center, which is not observed in complexes with *ortho* substituted ligands.

Our previous studies resulted in determination of basicity parameters of XPy's decreasing in the following order: 4-MePy (the strongest base) > 2-MePy > 3-MePy > Py > 3-ClPy > 2-ClPy (the weakest base). It might be expected that nucleophilicity and basicity of XPy would have a great impact on the Pd–N length. Pd–N distances are presented in Table 2, but, surprisingly, we do not observe a direct correlation between ligand basicity and Pd–N bond length. The difference between Pd–N distances for investigated complexes are too small and one can state that Pd–N (2.010–2.043 Å) lengths are similar for all the complexes **I–VI**. The only observation is that Pd–N distances are slightly longer for complexes with MePy compared to complexes with ClPy and that this difference can be explained by the greater contribution of back-donation of electrons from the central atom into ClPy than into MePy, related to the inductive effect of chlorine atoms.[34] As far as N–C length is concerned, the distance between N and C (substituted) in complex **V** is 5% shorter than the length of N–C (C-unsubstituted). It can also be explained by the inductive effect of the chlorine substituent which decreases the distance between N and C (substituted) (see the structure in Fig. 1C).

The presence of an *ortho* substituent in the pyridine ring is manifested by increasing the Pd–N distance in $PdCl_2(2\text{-XPy})_2$ as observed for **II** (Table 2) and for **V** (Table 2). Except for this "effect of *ortho* group", the introduction of methyl or chlorine in the *ortho* position of the pyridine ligand causes differences in the Pd–N–C bond angles in **II** and **V**.

Because of the symmetric disposition of methyl groups in 4-MePy ligands (complex **IV**) the bond angles Pd–N–C(1) and Pd–N–C(5) in this complex are equal (120.7 ± 0.2°) making compound **IV** more similar to *trans*-dichlorobis(pyridine)palladium(II), while in complex **III** a slight (*ca.* 2°) difference between Pd–N–C(1) and Pd–N–C(5) is observed (see Table 2). Another deviation of complexes with *ortho* substituted pyridines from the rest of investigated compounds is that the dihedral angles between the ligands are about 18° for 2-XPy while they are 0° for complexes containing 3- and 4-XPy. We suppose that the 2-XPy rings are not in one plane because of the packing effect.

Concluding this section, the nature and position of substituents in the aromatic ring is important to the structure of $PdCl_2(XPy)_2$ complexes. We observed a decrease in the distances between selected atoms in complexes with X = Cl compared to compounds with X = CH_3. In addition, the introduction of X (= Cl, CH_3) to the *ortho* position increases the Pd–N length and C–N–Pd angle values, however, we did not find a direct correlation between the basicity of the ligand and the Pd–N distance.

UV-Vis of XPy ligands and $PdCl_2(XPy)_2$ complexes

The absorption maxima and molar extinction coefficients ε ($dm^3\ mol^{-1}\ cm^{-1}$) of XPy ligands dissolved in acetonitrile are summarized in Table 3 and the spectra of the ligands are presented in Fig. 2. All spectra exhibit an intense band at 250–270 nm due to π–π^* transitions in the pyridine ring, in accordance with the spectra of methylpyridines measured in 1,2-dichloroethane[35] and halopyridines (in heptane).[36] The π–π^* bands are accompanied by a shoulder on the low energy side corresponding to n–π^* transitions of the C=N chromophore.[35] Strong charge transfer π–π^* and n–π^* transitions are partially overlapped and one band (220–290 nm) is observed instead of two separated bands.[37]

For 2-or 3-substituted pyridines the π–π^* and n–π^* bands show subtle (a few nanometres) red shifts in the visible region compared to the spectrum of unsubstituted pyridine. This effect, observed for all investigated pyridines, indicates that the energy of π–π^* and n–π^* transitions is greatly dependent on the position of a substituent, which is in agreement with the results reported by others.[38,39] The nature of the substituent also influences the energy of these transitions and an electron-withdrawing substituent (*e.g.*, chlorine) shifts the bands to a lower energy region, probably due to the relative destabilization of the π levels of pyridine ring.[40] The wavelength of absorption maximum, λ_{max}, increases in the order:

Table 3 UV-Vis spectroscopic features in acetonitrile for the free XPy ligands described in the present work

No	XPy	λ (nm)	ε^a (10^3 dm^3 mol^{-1} cm^{-1})	Energy (10^{-19} J)	Assignment
1	Py	251	2.87	7.93	—
		256	2.81	7.77	$\pi \rightarrow \pi^*$
		261	2.56	7.62	$n \rightarrow \pi^*$
2	2-MePy	256	3.73	7.77	—
		262	3.88	7.59	$\pi \rightarrow \pi^*$
		268	2.83	7.42	$n \rightarrow \pi^*$
3	3-MePy	258	3.73	7.71	—
		263	3.88	7.56	$\pi \rightarrow \pi^*$
		269	3.41	7.39	$n \rightarrow \pi^*$
4	4-MePy	255	3.76	7.80	$\pi \rightarrow \pi^*$
		261	3.40	7.62	$n \rightarrow \pi^*$
5	2-ClPy	257	4.07	7.74	—
		263	4.83	7.56	$\pi \rightarrow \pi^*$
		270	3.31	7.37	$n \rightarrow \pi^*$
6	3-ClPy	261	3.25	7.62	—
		266	3.49	7.48	$\pi \rightarrow \pi^*$
		272	2.55	7.31	$n \rightarrow \pi^*$

[a] ε is molar extinction coefficient

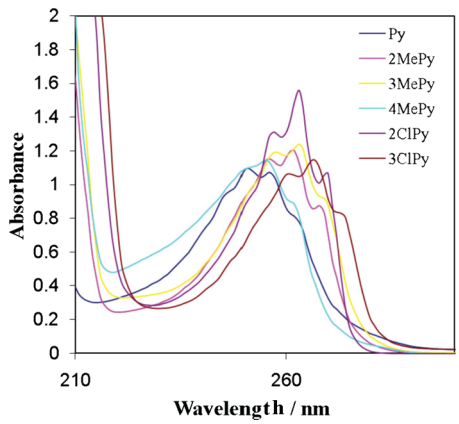

Fig. 2 UV-Vis spectra of free XPy ligands (full size plots of UV-Vis spectra are also presented in ESI†).

4MePy ≤ Py < 2-MePy ≤ 3-MePy = 2-Cl < 3-Cl in agreement with the results found in the literature.[35,36]

Having the UV-Vis spectra recorded for XPy ligands, we also carried out the UV-Vis measurements of Pd(II) complexes **I–VI** in acetonitrile and the results are listed in Table 4. The bands within 220–300 nm region are caused by intra-ligand π–$\pi^*$and n–π^* transitions. In each spectrum a n–π^* transition band is also observed as a shoulder on the π–π^* band, analogously to the spectra of free XPy's (see Fig. 3a). For complexes, a hipsochromic shift (24–34 nm) of π–π^* bands and bathochromic shift of n–π^* bands are observed and the intensities of π–π^* bands are about ten times higher than for free XPy (ε is about 10^4, while for free ligands it is 10^3 dm^3 mol^{-1} cm^{-1}). Another difference between the spectra of ligands and the spectra of complexes is a broadening of π–π^* and n–π^* bands for complexes, probably due to the contribution of π–π^* transitions in which chlorine ligands are involved. Also in this case the π–π^* bands energies are much more dependent on the substituent position in the pyridine ring than on the nature of substituents itself.

The presence of a central Pd atom in the complexes is manifested by two absorption bands at 300–400 nm corresponding to dπ–π^*

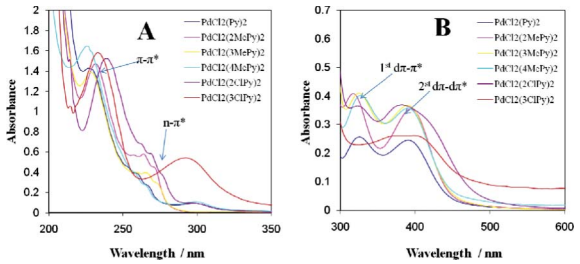

Fig. 3 UV-Vis spectra of $PdCl_2(XPy)_2$ complexes (full size plots of UV-Vis spectra are also presented in ESI†).

transitions.[41] Intensities of these transitions are smaller than the intensities of π–π^*, thus, in order to clearly observe them, the more concentrated solutions of $PdCl_2(XPy)_2$ in acetonitrile were applied (see details in Fig. 3b).

All investigated complexes are diamagnetic square-planar compounds, for which three spin-allowed d-d transitions are expected to occur, corresponding to $^1A_{1g} \rightarrow {}^1A_{2g}$, $^1A_{1g} \rightarrow {}^1B_{1g}$ and $^1A_{1g} \rightarrow {}^1E_g$, however, strong d$\pi$–$\pi^*$ or intra-ligand transitions may prevent the observation of these d-d bands.[42–45] Besides, d-d bands could not be observed because the electronic spectra of all complexes were recorded in solution.[5,46]

In summary to this section, the absorption spectra of free XPy ligands show that the energies of π–π^* and n–π^* transitions depend on the position and nature of the X substituent in the XPy ring. After complexation a hipsochromic shift (24–34 nm) of π–π^* and bathochromic shift of n–π^* bands are observed. The UV-Vis spectra of $PdCl_2(XPy)_2$ confirm the square planar coordination geometry of complexes **I–VI**, for which two dπ–π^* transitions are expected.

Theoretical calculations

Two absorption bands assigned as dπ–π^* (in experimentally obtained spectra, see Fig. 3b) can be related to either MLCT (*metal-to-ligand charge transfer*) or LMCT (*ligand-to-metal charge transfer*) transitions.[5,37,45,47] Therefore, the UV-Vis spectra of three selected complexes with ligands without *ortho* substituents: complex **I**, **III** and **VI** have been interpreted by TD-DFT calculations to understand the origin of dπ–π^* transitions. Our calculations indicate that the transition from Pd to XPy (M→L) is favored, which is consistent with the literature data.[37,48,49] The first theoretical dπ–π^* transition occurs at values 320 nm, 319 nm and 330 nm for **I**, **III** and **VI**, respectively (see Table 5). The most important frontier orbitals involved in the first dπ–π^* transitions are the highest occupied molecular orbitals H-1 (HOMO-1) and the lowest unoccupied molecular orbitals L+1 (LUMO+1) in all three complexes (**I**, **III**, **VI**). The contributions of each part of these complexes are listed in Table 6. Orbital H-1 is mainly located at the chlorine ligands with a contribution from the Pd centre whereas orbital L+1 is mostly centered at XPy ligands. The shapes of these orbitals are presented in Fig. 4 for $PdCl_2$ complex with 3-MePy (see ESI† for complexes **I** and **VI**). Other important frontier orbitals are H-3 (HOMO-3, placed at chlorine atoms with some contribution from the palladium atom and pyridine ligands) and LUMO (mainly located at the Pd centre). These results indicate that the Pd-to-XPy charge transfer assigned as MLCT is preceded

Table 4 UV-Vis spectroscopic features in acetonitrile for the $PdCl_2(XPy)_2$ complexes described in the present work

No	Compound $PdCl_2(XPy)_2$ (X = H, Cl, CH_3)	λ (nm)	ε^a ($dm^3\ mol^{-1}\ cm^{-1}$)	Energy (10^{-19} J)	Assignment
1	$PdCl_2(Py)_2$	226	$3.67*10^3$	8.80	$\pi \rightarrow \pi^*$
		298	$2.46*10^2$	6.67	$n \rightarrow \pi^*$
		326	$2.54*10^1$	6.10	$d\pi \rightarrow \pi^*$
		391	$2.43*10^1$	5.09	$d\pi \rightarrow \pi^*$
2	$PdCl_2(2\text{-}MePy)_2$	231	$2.57*10^4$	8.57	$\pi \rightarrow \pi^*$
		270	$1.02*10^4$	7.53	$n \rightarrow \pi^*$
		317	$1.86*10^2$	6.27	$d\pi \rightarrow \pi^*$
		394	$1.61*10^2$	5.05	$d\pi \rightarrow \pi^*$
3	$PdCl_2(3\text{-}MePy)_2$	229	$2.93*10^4$	8.69	$\pi \rightarrow \pi^*$
		273	$8.22*10^3$	7.51	$n \rightarrow \pi^*$
		325	$1.87*10^2$	6.12	$d\pi \rightarrow \pi^*$
		391	$1.67*10^2$	5.09	$d\pi \rightarrow \pi^*$
4	$PdCl_2(4\text{-}MePy)_2$	226	$1.95*10^4$	8.80	$\pi \rightarrow \pi^*$
		298	$1.32*10^3$	6.67	$n \rightarrow \pi^*$
		327	$1.83*10^2$	6.08	$d\pi \rightarrow \pi^*$
		391	$1.62*10^2$	5.09	$d\pi \rightarrow \pi^*$
5	$PdCl_2(2\text{-}ClPy)_2$	239	$2.01*10^4$	8.32	$\pi \rightarrow \pi^*$
		296	$1.28*10^3$	6.72	$n \rightarrow \pi^*$
		317	$1.81*10^2$	6.28	$d\pi \rightarrow \pi^*$
		382	$1.87*10^2$	5.21	$d\pi \rightarrow \pi^*$
6	$PdCl_2(3\text{-}ClPy)_2$	233	$2.08*10^4$	8.54	$\pi \rightarrow \pi^*$
		292	$7.13*10^3$	6.81	$n \rightarrow \pi^*$
		375	$3.98*10^2$	5.30	$d\pi \rightarrow \pi^*$
		397	$3.98*10^2$	5.00	$d\pi \rightarrow \pi^*$

[a] ε is molar extinction coefficient.

Table 5 Calculated values of wavelength, oscillator strength, symmetry, type of orbitals involved, and change of fragments contribution to the orbital during transition for selected electronic transitions

				The change of a fragment contribution to the orbital during transition		
Wave (nm)	Oscillator strength	Symmetry	Orbitals involved in the transition	Pd (%)	Cl (%)	XPy (%)
$PdCl_2(Py)_2$ **I**						
353.7	0.0004	Singlet-B	HOMO → L+1	36 → 0 (−36)	63 → 1 (−62)	2 → 99 (97)
328.7	0.0097	Singlet-A	H-3 → LUMO	10 → 49 (39)	85 → 28 (−57)	5 → 23 (18)
319.6	0.0131	Singlet-A	H-1 → L+1	21 → 0 (−21)	79 → 1 (−78)	0 → 99 (99)
$PdCl_2(3\text{-}MePy)_2$ **III**						
352.7	0.0004	Singlet-A	HOMO → L+1	35 → 0 (−35)	62 → 1 (−61)	3 → 99 (96)
329.5	0.0107	Singlet-A	H-3 → LUMO	11 → 49 (38)	79 → 28 (−51)	10 → 23 (13)
318.9	0.0141	Singlet-A	H-1 → L+1	22 → 1 (−21)	79 → 1 (−78)	0 → 99 (99)
$PdCl_2(3\text{-}ClPy)_2$ **V**						
367.2	0.0005	Singlet-AU	HOMO → L+1	34 → 0 (−34)	63 → 1 (−62)	2 → 99 (97)
335.4	0.0134	Singlet-AU	H-3 → LUMO	10 → 49 (39)	76 → 28 (−48)	14 → 22 (8)
330.4	0.0118	Singlet-AU	H-1 → L+1	20 → 1 (−19)	79 → 1 (−78)	1 → 98 (97)

by Cl-to-Pd transition occurring with lower energy (*i.e.* higher wavelength), in agreement with the literature data.[44]

The most important frontier orbitals involved in second $d\pi$–π^* transition are the occupied HOMO and the empty L+1 (LUMO+1). The calculated contributions of each part of $PdCl_2(Py)_2$; $PdCl_2(3\text{-}MePy)_2$ and $PdCl_2(3\text{-}ClPy)_2$ complexes are listed in Table 6 and examples of shapes of these orbitals for $PdCl_2(3\text{-}MePy)_2$ complex are given in Fig. 4. The HOMO is placed on chlorine ligands with contribution of Pd metal while the L+1 is located at XPy ligands. We do not observe such significant contribution of Cl-to-Pd charge transfer as for previously observed first higher energy $d\pi$–π^* transition. For each transition a contribution of XPy increases, therefore, the $d\pi$–π^* origins from MLCT (Pd-to-XPy). Predicted $d\pi$–π^* transitions are shown in Fig. 5. The predictions of $d\pi$–π^*, π–π^* and n–π^* transitions energies using TD-DFT calculations are consistent with experimental results (see ESI† for theoretical UV-Vis spectra for complexes **I**, **III** and **VI**). It can be concluded that the absorption spectra of $PdCl_2(XPy)_2$ complexes are dominated by intra-ligand (LL, ligand-to-ligand) π–π^* and n–π^* transitions, as well as MLCT (Pd-to-XPy) with CT contribution from chlorine atoms to palladium. To summarize this part of our research, on the basis of theoretical calculations for the first time we proved that the observed $d\pi$–π^* transitions for $PdCl_2(XPy)_2$ complexes in solutions result from MLCT (metal-to-ligand charge transfer) with contribution of chlorine atoms to palladium charge transfer.

Cytotoxic activity

Apart from the analyses of the structural and chemical properties of $PdCl_2(XPy)_2$ complexes, we performed preliminary analyses of

Table 6 Composition of selected frontier molecular orbitals in terms of Pd, Cl and XPy fragments

MO	*E*(eV)	Symmetry	Pd (%)	Cl (%)	XPy (%)
$PdCl_2(Py)_2$ **I**					
L+1	−1.99	B	0	0	99
LUMO	**−2.32**	**A**	**49**	**28**	**22**
HOMO	**−6.25**	**A**	**36**	**63**	**2**
H-1	−6.61	B	21	79	0
H-3	−7.14	A	10	85	5
$PdCl_2(3\text{-}MePy)_2$ **III**					
L+1	−1.89	A	0	0	99
LUMO	**−2.2**	**A**	**49**	**28**	**22**
HOMO	**−6.15**	**A**	**35**	**62**	**3**
H-1	−6.5	A	22	79	0
H-3	−7	A	11	80	9
$PdCl_2(3\text{-}ClPy)_2$ **V**					
L+1	−2.35	Au	0	0	99
LUMO	**−2.61**	**Ag**	**50**	**29**	**21**
HOMO	**−6.48**	**Ag**	**34**	**63**	**2**
H-1	−6.83	Ag	20	79	1
H-3	−7.33	Au	10	77	13

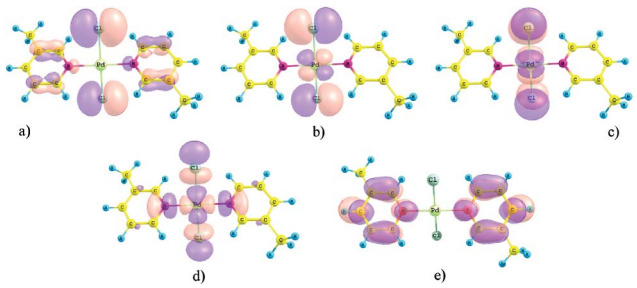

Fig. 4 Frontier orbitals involved in dπ–π* transitions in $PdCl_2(3\text{-}MePy)_2$: HOMO-3, HOMO-1, HOMO, LUMO and LUMO+1: a) HOMO-3 Cl centered (involved in first dπ–π*), b) HOMO-1 Cl-Pd centered (involved in first dπ–π*), c) HOMO Cl-Pd centered (involved in second dπ–π*), d) LUMO Pd-Cl-3MePy centered (involved in first dπ–π*), e) LUMO+1 3-MePy centered (involved in first and second dπ–π*).

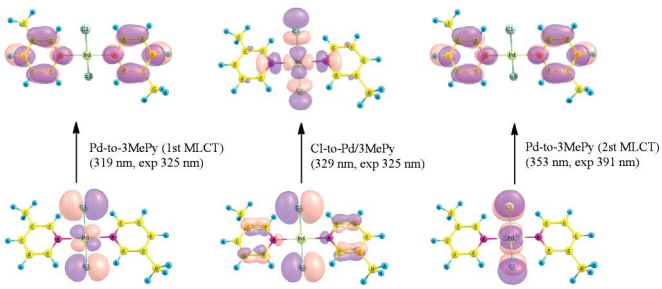

Fig. 5 Visualisation of dπ–π* transitions in $PdCl_2(3\text{-}MePy)_2$.

their cytotoxicity. For these studies three established cell lines were selected. Human breast cancer cell line MCF7, human prostate cancer cell line PC3, and human T-cell lymphoblast-like cell line CCRF. Cells were incubated in the culture medium containing complexes **I–VI** or cisplatin in selected concentrations either for 48 h (MCF7) or 72 h (MCF7, PC3, CCRF). Next, MTT[50,51] assay allowing the analysis of cell viability, was performed. For cisplatin the IC_{50} was determined as 3 μM, for CCRF cells. Poor solubility of complexes in **I–VI** allowed us to do a limited comparison of activity of our Pd(II) complexes with the activity of cisplatin, however, even for concentrations below IC_{50} the results are interesting. The viability of control CCRF cells, *i.e.* cultured for 72 h in the medium without any additions of tested compounds was assumed to be 100% (which is the average of four measurements). Some of the $PdCl_2(XPy)_2$ complexes at concentration below 1 μM were significantly more cytotoxic than cisplatin (see Fig. 6). Compounds **II** and **III** used at concentrations of about 0.1 μM reduced the viability to 60%, *i.e.* had significantly higher effect than measured for cisplatin (90% of surviving cells). Incubation with two other compounds **I** and **VI** resulted in 80% of cells surviving the treatment, *i.e.* they were still more toxic than cisplatin. At concentration about 1 μM complexes **I** and **II** showed very high cytotoxicity about 60%, while results obtained for **III** were not statistically significant. Experiments with two other cell lines PC3 and MCF7 indicated moderate cytotoxicity of complexes with MePy: **II**, **III** and **IV** (slightly higher than $PdCl_2$ with Py and ClPy against PC3). 48 h long incubation of MCF7 cells in all $PdCl_2(XPy)_2$ complexes did not result in the decrease of their survival, while compounds **II**, **IV** and **VI** showed low cytotoxic activity against MCF after 72 h.

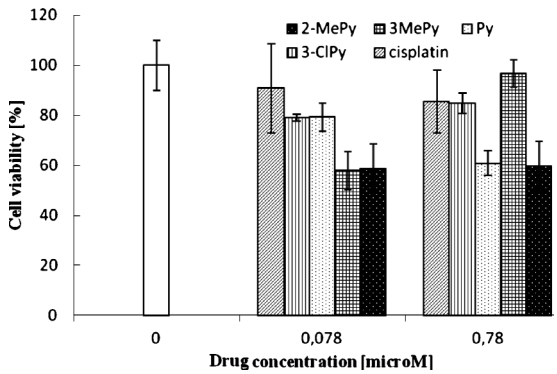

Fig. 6 Cytotoxicity of selected complexes (**I, II, III, VI**) and cisplatin (cisDDP) against CCRF cells. The control sample is marked as 0% concentration of drug.

Based on the results of the MTT test, significant differences have been found in the cytotoxic activity of all the complexes depending on the structure of the $PdCl_2(XPy)_2$ and depending on the cell line used for the experiments. Palladium complexes were the most active against the CCRF cell line and less or even no cytotoxic effect was observed for PC3 cells. The cytotoxic activity depends on the nature and position of substituents in the pyridine ring: complexes with MePy have increased cytotoxic activity compared to unsubstituted pyridine ligands. These findings are in accordance with those obtained by Huq *et al.*[13] for a series of $PdCl_2$ complexes with hydroxypyridines against A2780 cells. They reported that the cytotoxic effect on cells viability depended on the position of OH in the pyridine ring and decreased in the following order: 2-OH-pyridine > 3-OH-pyridine > 4-OH-pyridine.[13]

Experimental section

Materials

$PdCl_2$ was used as received. Pyridine (Py), substituted pyridines (2-MePy, 3-MePy, 4-MePy, 2-ClPy, 3-ClPy), acetonirile and acetone were distilled (or fractionally distilled) over CaH_2 and stored under argon. Human breast cancer cell line MCF7, human prostate

cancer cell line PC3 and human T-cell lymphoblast-like cell line CCRF-SB were purchased from ATCC, Manassas, VA. RPMI-1640 medium, Iscove's Modified Dulbecco's Medium (IMDM), fetal bovine serum, antibiotic-antimycotic solution (100IU ml^{-1} penicillin, 100 μg ml^{-1} streptomycin, 250 ng ml^{-1} amphotericin), glucose, MEM Non-essential Amino Acid Solution (100*), L-glutamine were purchased from Sigma Aldrich.

Synthesis of $PdCl_2(XPy)_2$ (compounds I–VI)

The procedure has been described elsewhere.[1] Palladium chloride complexes with pyridines were prepared under argon. $PdCl_2$ (1.128 mmol) was placed in a 10 ml flask equipped with a magnetic stirrer and 2.26 mmol of Py or substituted XPy in 10 ml acetonitrile were added. Reaction was carried out at room temperature for 24 h.

X-ray structure determinations

All measurements of crystal structure were performed on a KM4CCD κ-axis diffractometer with graphite-monochromated Mo-Kα radiation. The crystals were positioned at 62 mm from the CCD camera. 1600 frames were measured at 0.5° intervals with a counting time of 11 s. The data were corrected for Lorentz and polarization effects. Empirical correction for absorption was applied.[52] Data reduction and analysis were carried out with the Oxford Diffraction programs.[53] The structures were solved by direct methods[54] and refined using SHELXL.[55] The refinement was based on F^2 for all reflections except those with very negative F^2. Weighted R factors wR and all goodness-of-fit S values are based on F^2. Conventional R factors are based on F with F set to zero for negative F^2. The $F_0^2 > 2\sigma(F_0^2)$ criterion was used only for calculating R factors and is not relevant to the choice of reflections for the refinement. The R factors based on F^2 are about twice as large as those based on F. All hydrogen atoms were located geometrically and their positions were refined. Temperature factors for some hydrogen atoms were fixed. Scattering factors were taken from Tables 6.1.1.4 and 4.2.4.2.[56] The crystallographic data for the complexes are summarized in Table 1.

UV-Vis measurements

Electronic spectra of XPy ligands and $PdCl_2(XPy)_2$ complexes (**I–VI**) were recorded on a Cary 50 UV-Vis Spectrophotometer using acetonitrile as a solvent in the 200–800 nm range with a 1 cm quartz cell. Baseline was measured for acetonirile.

TDDFT calculations

All calculations were performed using Gaussian 03 software[57] with the B3LYP functional.[58,59] Three basis sets were employed. For palladium atom, the MWB28 energy-consistent Stuttgart-Dresden pseudo-relativistic basis set was used.[60] In this case 60 core electrons were replaced by Effective Core Potentials (ECP) and the 18 valence electrons were treated explicitly. For all other atoms standard Pople-style basis sets were employed: for geometry optimizations 6-31G(d)[61] and for TDDFT calculations 6-311+G(d).[62] Optimization of geometric parameters of all complexes were followed by frequency check to ensure that the stationary points obtained are true minima on the potential energy surface. For each optimized structure a total of 50 singlet excited states and their corresponding oscilator strengths were simulated *via* TDDFT methodology.[63] The results were analyzed using GaussSum 2.2.5 package[64] and visualized using ChemCraft program.[65]

Cytotoxic activity

MCF7 cells (from ATCC, USA) were grown in Iscove's Modified Dulbecco's Medium containing L-glutamine (IMDM, Sigma-Aldrich) supplemented with a 10% heat inactivated fetal bovine serum (Sigma-Aldrich), antibiotics (100 IU ml^{-1} penicillin, 100 μg ml^{-1} streptomycin, 250 ng ml^{-1} amphotericin, (Sigma-Aldrich), 0.4% glucose (Sigma-Aldrich) and nonessential amino acids (1×, Sigma-Aldrich). PC3 and CCRF cell lines (collected from ATCC, USA) were grown in RPMI-1640 medium (Sigma-Aldrich) supplemented with nonessential amino acids (1×), antibiotics (100 IU ml^{-1} penicillin, 100 μg ml^{-1} streptomycin, 250 ng ml^{-1} amphotericin), 0.4% glucose, L-glutamine and heat inactivated bovine serum (10% for PC3 and 20% for CCRF-SB). Cells were grown at 37 °C in a humidified atmosphere containing 5% CO_2. MCF7 and PC3 cells were treated with $PdCl_2(XPy)_2$ (**I–VI**) and cisplatin at the concentration range 0.6–85 μM, depending on the solubility of the used complex. CCRF cells were treated with compounds (**I–VI**) and cisplatin at the concentration range 0.002–100 μM.

The cytotoxic properties of the compounds were evaluated by MTT test.[49,50] The assay measures the amount of formazan produced from 3-(4,5-dimethylthiazol-2-yl)-2,5-diphenyltetrazolium bromide (assigned as MTT) by living cells present in the culture. Cells were seeded in a 96-well plate at density 5×10^4 cells ml^{-1} (MCF7), 6×10^4 cells ml^{-1} (PC3) and 5×10^5 cells ml^{-1} (CCRF). Next, the solutions of compounds prepared in dimethylformamide (DMF)/growth medium (appropriate for cell line used in the experiment—IMDM or RPMI) were added—the concentration of DMF was 1% (v/v), and once (for low soluble compound) the concentration of DMF reached 2% (v/v). To the control samples of cells the DMF/growth medium without any other additives were used. Cells were incubated with compounds for 48 h (MCF7 cells) and 72 h (all cell lines). After incubation time, cells were washed in PBS and, subsequently, to each well 0.25 mg ml^{-1} of MTT was applied. After 3 h incubation at 37 °C, isopropanol was added to dissolve formazan crystals (formed from MTT). The absorbance (at 570 nm) was measured with a spectrophotometer PowerWave XS (Biotek Instruments). The results describing viability of cells are present in this paper as a mean of 4 repetitions. Standard deviations (which are shown in Fig. 6) were calculated from four measurements and the t-Student test was performed with reference to the control sample at the confidence level $\rho < 0.05$.

Conclusions

In the present work the X-ray characterization, electronic properties and TD-DFT calculations for $PdCl_2(XPy)_2$ complexes (where: Py = pyridine and X = H, Cl or CH_3) are discussed. We also studied substituent effects on cytotoxic properties of Pd(II) compounds by monitoring anticancer activity of the complexes against CCRF, PC3 and Mcf7 cell lines. We report that the nature and position of substituents in the aromatic ring is important to the structure of $PdCl_2(XPy)_2$ complexes. The absorption spectra

of free XPy ligands show that the energies of π–π^* and n–π^* transitions depend on the position and nature of the X substituent in the XPy ring. After complexation a hipsochromic shift of π–π^* and bathochromic shift of n–π^* bands are observed. The UV-Vis spectra of $PdCl_2(XPy)_2$ confirm the square planar coordination geometry of complexes **I–VI**, for which two dπ–π^* transitions are expected. On the basis of theoretical calculations for the first time we prove that dπ–π^* transitions in solutions of $PdCl_2(XPy)_2$ complexes result from MLCT (metal-to-ligand charge transfer) with contribution of chlorine atoms to palladium and pyridine (XPy) charge transfer. Anticancer activity depends on the nature and position of substituents in the pyridine ring of the compound: complexes with X = MePy have increased cytotoxic activity compared with X = Py ligands.

Acknowledgements

A. Krogul is thankful for the Mazowian Doctoral Scholarship in 2011. This work was partially supported by the Ministry of Science and Higher Education of Poland, grant No. N N507 452937.

Notes and references

1 A. Krogul, J. Skupińska and G. Litwinienko, *J. Mol. Catal. A: Chem.*, 2011, **337**, 9.
2 F. Paul, *Coord. Chem. Rev.*, 2000, **203**, 269.
3 F. Ragaini and S. Cenini, *J. Mol. Catal. A: Chem.*, 1996, **109**, 1.
4 A. Aeby, A. Gsponer and G. Consiglio, *J. Am. Chem. Soc.*, 1998, **120**, 11000.
5 A. Kilic, D. Kilinc, E. Tas, I. Yilmaz, M. Durgun, I. Ozdemir and S. Yasar, *J. Organomet. Chem.*, 2010, **695**, 697.
6 C. Y. Liao, K. T. Chan, J. Y. Zeng, C. H. Hu, C. Y. Tu and H. M. Lee, *Organometallics*, 2007, **26**, 1692.
7 A. Garoufis, S. K. Hadjikakou and N. Hadjiliadis, *Coord. Chem. Rev.*, 2009, **253**, 1384.
8 M. A. Fuertes, C. Alonso and J. M. Pérez, *Chem. Rev.*, 2003, **103**, 645.
9 A. P. Neves, G. B. da Silva, M. D. Vargas, C. B. Pinheiro, L. C. Visentin, J. D. B. M. Filho, A. J. Araújo, L. V. Costa-Lotufo, C. Pessoa and M. O. de Moraes, *Dalton Trans.*, 2010, **39**, 10203.
10 J. Reedijk, *Proc. Natl. Acad. Sci. U. S. A.*, 2003, **100**, 3611.
11 E. Budzisz, M. Malecka, B. K. Keppler, V. B. Arion, G. Andrijewski, U. Krajewska and M. Rozalski, *Eur. J. Inorg. Chem.*, 2007, 3728.
12 R. A. Michelin, P. Sgarbossa, S. Mazzega Sbovata, V. Gandin, C. Marzano and R. Bertani, *ChemMedChem*, 2011, **6**, 1172.
13 F. Huq, H. Tayyem, P. Beale and J. Q. Yu, *J. Inorg. Biochem.*, 2007, **101**, 30.
14 J. M. Vujić, M. Cvijović, G. N. Kaluderović, M. Milovanović, B. B. Zmejkovski, V. Volarević, N. Arsenijević, T. J. Sabo and S. R. Trifunović, *Eur. J. Med. Chem.*, 2010, **45**, 3601.
15 Z. D. Bugarčić, B. Petrović and E. Zangrando, *Inorg. Chim. Acta*, 2004, **357**, 2650.
16 K. Fukui, *Science*, 1982, **218**, 747.
17 A. V. Chuchuryukin, P. A. Chase, A. M. Mills, M. Lutz, A. L. Spek, G. P. M. van Klink and G. van Koten, *Inorg. Chem.*, 2006, **45**, 2045.
18 D. Jaganyi, F. Tiba, O. Q. Munro, B. Petrović and D.Ž. Bugarčić, *Dalton Trans.*, 2006, 2943.
19 B. A. Blight, J. A. Wisner and M. C. Jennings, *Inorg. Chem.*, 2009, **48**, 1920.
20 P. O. Dunstan, *Thermochim. Acta*, 2007, **456**, 32.
21 M. Schlosser and F. Mongin, *Chem. Soc. Rev.*, 2007, **36**, 1161.
22 M. L. Dell'Arciprete, C. J. Cobos, J. P. Furlong, D. O. Mártire and M. C. Gonzalez, *ChemPhysChem*, 2007, **8**, 2498.
23 L. Pazderski, E. Szłyk, J. Sitkowski, B. Kamieński, L. Kozerski, J. Toušek and R. Marek, *Magn. Reson. Chem.*, 2006, **44**, 163.
24 J. Skupińska and M. Karpińska, *Appl. Catal., A*, 2004, **267**, 59.
25 J. Skupińska, M. Karpińska, M. Ołówek and T. Kasprzycka-Guttman, *Cent. Eur. J. Chem.*, 2005, **3**, 28.
26 J. Skupińska and M. Karpińska, *J. Mol. Catal. A: Chem.*, 2000, **161**, 69.
27 J. Skupińska, A. Żukowska and A. Chajewski, *React. Kinet. Catal. Lett.*, 2001, **72**, 21.
28 J. Skupińska, M. Karpińska, L. Wachowski and M. Hofman, *React. Kinet. Catal. Lett.*, 2004, **82**, 311.
29 M. Karpińska, P. Baran and J. Skupińska, *Pol. J. Chem.*, 2008, **82**, 1105.
30 J. Skupińska, M. Karpińska and M. Ołówek, *Appl. Catal., A*, 2005, **284**, 147.
31 P. B. Viossat, *Acta Crystallogr., Sect. C: Cryst. Struct. Commun.*, 1993, **49**, 84.
32 M. C. Biagini, M. Ferrari, M. Lanfranchi, L. Marchiò and M. A. Pellinghelli, *J. Chem. Soc., Dalton Trans.*, 1999, 1575.
33 F. Zordan, L. Brammer and P. Sherwood, *J. Am. Chem. Soc.*, 2005, **127**, 5979.
34 D. Jaganyi, A. Hofmann and R. van Eldik, *Angew. Chem., Int. Ed.*, 2001, **40**, 1680.
35 T. Handa, Y. Utena, H. Yajima and T. Ishii, *J. Phys. Chem.*, 1986, **90**, 2589.
36 H. C. Brown and D. H. McDaniel, *J. Am. Chem. Soc.*, 1955, **77**, 3752.
37 A. K. Mishra, S. B. Mishra, N. Manav and N. K. Kaushik, *J. Therm. Anal. Calorim.*, 2007, **90**, 509.
38 H. C. Brown and X. R. Mihm, *J. Am. Chem. Soc.*, 1955, **77**, 1723.
39 J. H. Rush and H. Sponer, *J. Chem. Phys.*, 1952, **20**, 1847.
40 I. Serrano, X. Sala, E. Plantalech, M. Rodriguez, I. Romero, S. Jansat, M. Gómez, T. Parella, H. Stoeckli-Evans, X. Solans, M. Font-Bardia, B. Vidjayacoumar and A. Llobet, *Inorg. Chem.*, 2007, **46**, 5381.
41 S. B. Halligudi, K. N. Bhatt, N. H. Khan, R. I. Kurashy and K. Venkatsubramanian, *Polyhedron*, 1996, **15**, 2093.
42 G. Henrici-Olivé, S. Olivé, *Coordination and Catalysis*, Verlag Chemie, Weinheim, 1977.
43 M. Čurić, L. Tušek-Božić and P. Traldi, *Polyhedron*, 1998, **17**, 531.
44 S. S. Kandil, S. M. A. Katib and N. H. M. Yarkandi, *Transition Met. Chem.*, 2007, **32**, 791.
45 S. Sönmez, M. Çelebi, A. Levent, I. Berber and Z. Şentürk, *J. Coord. Chem.*, 2010, **63**, 848.
46 V. Arun, N. Sridevi, P. P. Robinson, S. Manju and K. K. M. Yusuff, *J. Mol. Catal. A: Chem.*, 2009, **304**, 191.
47 D. Kovala-Demertzi, M. A. Demertzis, J. R. Miller, C. S. Frampton, J. P. Jasinski and D. X. West, *J. Inorg. Biochem.*, 2002, **92**, 137–140.
48 A. R. Lathem, V. C. Hascall and H. B. Gray, *Inorg. Chem.*, 1965, **4**, 788–792.
49 E. Guney, V. T. Yilmaz and C. Kazak, *Polyhedron*, 2010, **29**, 1285–1290.
50 F. Denizot and R. Lang, *J. Immunol. Methods*, 1986, **89**, 271–277.
51 J. Carmichael, W. G. DeGraff, A. F. Gazdar, J. D. Minna and J. B. Mitchell, *Cancer Res.*, 1987, **47**, 936.
52 CrysAlis RED, Oxford Diffraction Ltd.,Version 1.171.28cycle2 beta (release 25-10-2005 CrysAlis171 .NET) (compiled Oct 25 2005,08:50 : 05). Empirical absorption correction using spherical harmonics, implemented in SCALE3 ABSPACK scaling algorithm.
53 CrysAlis CCD, Oxford Diffraction Ltd., Version 1.171.28cycle2 beta CrysAlis RED, Oxford Diffraction Ltd.,Version 1.171.28cycle2 beta.
54 G. M. Sheldrick, *Acta Crystallogr., Sect. A: Found. Crystallogr.*, 1990, **46**, 467–473.
55 G. M. Sheldrick, *SHELXL93. Program for the Refinement of Crystal Structures*, Univ. of Göttingen, Germany.
56 International Tables for Crystallography, Ed. A. J. C. Wilson, Kluwer, Dordrecht, Vol.C. 1992.
57 M. J. Frisch *et al.*, *GAUSSIAN 03, Revision E.01*, Gaussian Inc., Wallingford, CT, 2004.
58 A. D. Becke, *J. Chem. Phys.*, 1993, **98**, 5648.
59 P. J. Stephens, F. J. Devlin, C. F. Chabalowski and M. J. Frisch, *J. Phys. Chem.*, 1994, **98**, 11623.
60 D. Andrae, U. Haussermann, M. Dolg, H. Stoll and H. Preuss, *Theor. Chim. Acta*, 1990, **77**, 123.
61 W. J. Hehre, R. Ditchfield and J. A. Pople, *J. Chem. Phys.*, 1972, **56**, 2257.
62 A. D. McLean and G. S. Chandler, *J. Chem. Phys.*, 1980, **72**, 5639.
63 R. E. Stratmann, G. E. Scuseria and M. J. Frisch, *J. Chem. Phys.*, 1998, **109**, 8218.
64 N. M. O'Boyle, A. L. Tenderholt and K. M. Langner, *J. Comput. Chem.*, 2008, **29**, 839–845.
65 http://www.chemcraftprog.com.

